

2

Photoionization Equilibrium

2.1 Introduction

Emission nebulae result from the photoionization of a diffuse gas cloud by ultraviolet photons from a hot “exciting” star or from a cluster of exciting stars. The ionization equilibrium at each point in the nebula is fixed by the balance between photoionizations and recombinations of electrons with the ions. Since hydrogen is the most abundant element, we can get a first idealized approximation to the structure of a nebula by considering a pure H cloud surrounding a single hot star. The ionization equilibrium equation is:

$$\begin{aligned} n(\text{H}^0) \int_{\nu_0}^{\infty} \frac{4\pi J_{\nu}}{h\nu} a_{\nu}(\text{H}^0) d\nu &= n(\text{H}^0) \int_{\nu_0}^{\infty} \phi_{\nu} a_{\nu}(\text{H}^0) d\nu = n(\text{H}^0) \Gamma(\text{H}^0) \\ &= n_e n_p \alpha(\text{H}^0, T) [\text{cm}^{-3} \text{s}^{-1}] \end{aligned} \quad (2.1)$$

where J_{ν} is the mean intensity of radiation (in energy units per unit area, per unit time, per unit solid angle, per unit frequency interval) at the point. Thus $\phi_{\nu} = 4\pi J_{\nu}/h\nu$ is the number of incident photons per unit area, per unit time, per unit frequency interval, and $a_{\nu}(\text{H}^0)$ is the ionization cross section for H by photons with energy $h\nu$ (above the threshold $h\nu_0$); the integral [denoted by $\Gamma(\text{H}^0)$] therefore represents the number of photoionizations per H atom per unit time. The neutral atom, electron, and proton densities per unit volume are $n(\text{H}^0)$, n_e , and n_p , and $\alpha(\text{H}^0, T)$ is the recombination coefficient; so the right-hand side of the equation gives the number of recombinations per unit volume per unit time.

To a first approximation, the mean intensity J_{ν} [see Appendix 1 for definitions of it and other observed (or measured) quantities connected with radiation] is simply the radiation emitted by the star reduced by the inverse-square effect of geometrical dilution. Thus

$$4\pi J_{\nu} = \frac{R^2}{r^2} \pi F_{\nu}(0) = \frac{L_{\nu}}{4\pi r^2} [\text{erg cm}^{-2} \text{s}^{-1} \text{Hz}^{-1}], \quad (2.2)$$

where R is the radius of the star, $\pi F_\nu(0)$ is the flux at the surface of the star, r is the distance from the star to the point in question, and L_ν is the luminosity of the star per unit frequency interval.

At a typical point in a nebula, the ultraviolet radiation field is so intense that the H is almost completely ionized. Consider, for example, a point in an H II region, with density 10 H atoms and ions per cm^3 , 5 pc from a central O7.5 star with $T_* = 39,700$ K. We will examine the numerical values of all the other variables later, but for the moment, we can adopt the following very rough values:

$$Q(\text{H}^0) = \int_{\nu_0}^{\infty} \frac{L_\nu}{h\nu} d\nu \approx 1 \times 10^{49} \text{ [photons s}^{-1}\text{]};$$

$$a_\nu(\text{H}^0) \approx 6 \times 10^{-18} \text{ [cm}^2\text{]};$$

$$\int_{\nu_0}^{\infty} \frac{4\pi J_\nu}{h\nu} a_\nu(\text{H}^0) d\nu \approx 1 \times 10^{-8} = \tau_{ph}^{-1} \text{ [s}^{-1}\text{]};$$

$$\alpha(\text{H}^0, T) \approx 4 \times 10^{-13} \text{ [cm}^3 \text{s}^{-1}\text{]}$$

where τ_{ph} is the lifetime of the atom before photoionization. Substituting these values and taking ξ as the fraction of neutral H, that is, $n_e = n_p = (1 - \xi)n(\text{H})$ and $n(\text{H}^0) = \xi n(\text{H})$, where $n(\text{H}) = 10 \text{ cm}^{-3}$ is the density of H, we find $\xi \approx 4 \times 10^{-4}$; that is, H is very nearly completely ionized.

On the other hand, a finite source of ultraviolet photons cannot ionize an infinite volume, and therefore, if the star is in a sufficiently large gas cloud, there must be an outer edge to the ionized material. The thickness of this transition zone between ionized and neutral gas, since it is due to absorption, is approximately one mean free path of an ionizing photon $\{l \approx [n(\text{H}^0) \alpha_\nu]^{-1} \text{ cm}\}$. Using the same parameters as before, and taking $\xi = 0.5$, we find the thickness

$$d \approx \frac{1}{n(\text{H}^0) \alpha_\nu} \approx 0.1 \text{ pc},$$

or much smaller than the radius of the ionized nebula. Thus we have the picture of a nearly completely ionized "Strömgren sphere" or H II region, separated by a thin transition region from an outer neutral gas cloud or H I region. In the rest of this chapter we will explore this ionization structure in detail.

First we will examine the photoionization cross section and the recombination coefficients for H, and then use this information to calculate the structure of hypothetical pure H regions. Next we will consider the photoionization cross section and recombination coefficients for He, the second most abundant element, and then calculate more realistic models of H II regions, that take both H and He into account. Finally, we will extend our analysis to other, less abundant heavy elements; these often do not strongly affect the ionization structure of the nebula, but are always quite important in the thermal balance to be discussed in the next chapter.

2.2 Photoionization and Recombination of Hydrogen

Figure 2.1 is an energy-level diagram of H; the levels are marked with their quantum numbers n (principal quantum number) and L (angular momentum quantum number), and with S, P, D, F, \dots standing for $L = 0, 1, 2, 3, \dots$ in the conventional notation. Permitted transitions (which, for one-electron systems, must satisfy the selection rule $\Delta L = \pm 1$) are marked by solid lines in the figure. The transition probabilities $A(nL, n'L')$ of these lines are of order 10^4 to 10^8 s^{-1} , and the corresponding mean lifetimes of the excited levels,

$$\tau_{nL} = \frac{1}{\sum_{n' < n} \sum_{L' = L \pm 1} A_{nL, n'L'}}, \quad (2.3)$$

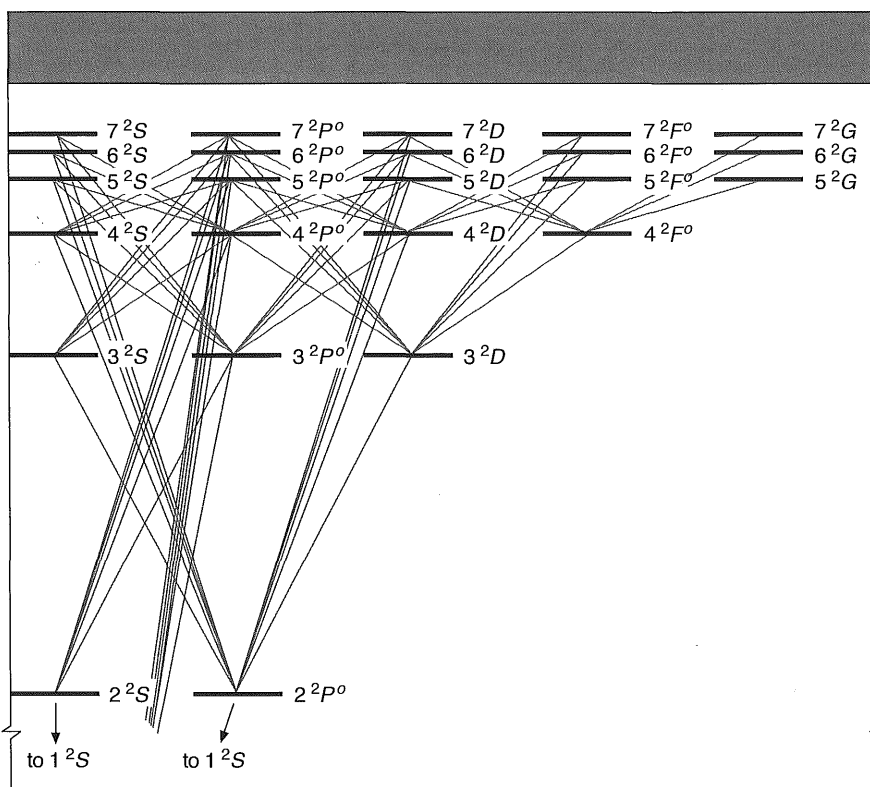


Figure 2.1

Partial energy-level diagram of H I, limited to $n \leq 7$ and $L \leq G$. Permitted radiative transitions to levels $n < 4$ are indicated by solid lines.

are therefore of order 10^{-4} to 10^{-8} s. The only exception is the 2^2S level, from which there are no allowed one-photon downward transitions. However, the transition $2^2S \rightarrow 1^2S$ does occur with the emission of two photons, and the probability of this process is $A(2^2S, 1^2S) = 8.23 \text{ s}^{-1}$, corresponding to a mean lifetime for the 2^2S level of 0.12 s. Even this lifetime is quite short compared with the mean lifetime of an H atom against photoionization, which has been estimated previously as $\tau_{ph} \approx 10^8$ s for the 1^2S level, and is of the same order of magnitude for the excited levels. Thus, to a very good approximation, we may consider that very nearly all the H^0 is in the 1^2S level, that photoionization from this level is balanced by recombination to all levels, and that recombination to any excited level is followed very quickly by radiative transitions downward, leading ultimately to the ground level. This basic approximation greatly simplifies calculations of physical conditions in gaseous nebulae.

The photoionization cross section for the 1^2S level of H^0 , or, in general, of a hydrogenic ion with nuclear charge Z , may be written in the form

$$a_\nu(Z) = \frac{A_0}{Z^2} \left(\frac{\nu_1}{\nu} \right)^4 \frac{\exp \{4 - [(4 \tan^{-1} \varepsilon) / \varepsilon]\}}{1 - \exp(-2\pi/\varepsilon)} [\text{cm}^2] \text{ for } \nu \geq \nu_1 \quad (2.4)$$

where

$$A_0 = \frac{2^9 \pi}{3e^4} \left(\frac{1}{137.0} \right) \pi a_0^2 = 6.30 \times 10^{-18} [\text{cm}^2],$$

$$\varepsilon = \sqrt{\frac{\nu}{\nu_1} - 1},$$

(with ε denoting the base of the natural logarithm, not the electron charge), and

$$h\nu_1 = Z^2 h\nu_0 = 13.6Z^2 \text{ eV}$$

is the threshold energy. This cross section is plotted in Figure 2.2, which shows that it drops off rapidly with energy, approximately as ν^{-3} not too far above the threshold, which, for H, is at $\nu_0 = 3.29 \times 10^{15} \text{ s}^{-1}$ or $\lambda_0 = 912 \text{ \AA}$, so that the higher-energy photons, on the average, penetrate further into neutral gas before they are absorbed.

The electrons produced by photoionization have an initial distribution of energies that depends on $J_\nu a_\nu / h\nu$. However, the cross section for elastic scattering collisions between electrons is quite large, of order $4\pi(e^2/mu^2)^2 \approx 10^{-13} \text{ cm}^2$, and these collisions tend to set up a Maxwell-Boltzmann energy distribution. The recombination cross section, and all the other cross sections involved in the nebulae, are so much smaller that, to a very good approximation, the electron-distribution function is Maxwellian, and therefore all collisional processes occur at rates fixed by the local

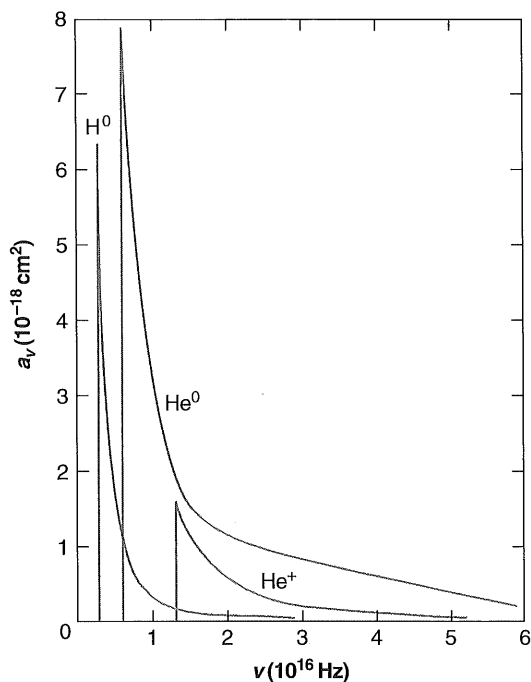


Figure 2.2

Photoionization absorption cross sections of H^0 , He^0 , and He^+ .

temperature defined by this Maxwellian. Therefore, the recombination coefficient of a specified term n^2L may be written

$$\alpha_{n^2L}(H^0, T) = \int_0^\infty u \sigma_{n^2L}(H^0, u) f(u) du \quad [\text{cm}^3 \text{s}^{-1}] \quad (2.5)$$

where

$$f(u) = \frac{4}{\sqrt{\pi}} \left(\frac{m}{2kT} \right)^{3/2} u^2 \exp(-mu^2/2kT) \quad (2.6)$$

is the Maxwell-Boltzmann distribution function for the electrons, and $\sigma_{n^2L}(H^0, u)$ is the recombination cross section to the term n^2L in H^0 for electrons with velocity u . These cross sections vary approximately as u^{-2} , and the recombination coefficients, which are proportional to $u\sigma$, therefore vary approximately as $T^{-1/2}$. A selection of numerical values of α_{n^2L} is given in Table 2.1. Since the mean electron velocities at

Table 2.1
Recombination coefficients (in $\text{cm}^3 \text{s}^{-1}$) $\alpha_n {}^2L$ for H

	5,000 K	10,000 K	20,000 K
$\alpha_1 {}^2S$	2.28×10^{-13}	1.58×10^{-13}	1.08×10^{-13}
$\alpha_2 {}^2S$	3.37×10^{-14}	2.34×10^{-14}	1.60×10^{-14}
$\alpha_2 {}^2P^o$	8.33×10^{-14}	5.35×10^{-14}	3.24×10^{-14}
$\alpha_3 {}^2S$	1.13×10^{-14}	7.81×10^{-15}	5.29×10^{-15}
$\alpha_3 {}^2P^o$	3.17×10^{-14}	2.04×10^{-14}	1.23×10^{-14}
$\alpha_3 {}^2D$	3.43×10^{-14}	1.73×10^{-14}	9.49×10^{-15}
$\alpha_4 {}^2S$	5.23×10^{-15}	3.59×10^{-15}	2.40×10^{-15}
$\alpha_4 {}^2P^o$	1.51×10^{-14}	9.66×10^{-15}	5.81×10^{-15}
$\alpha_4 {}^2D$	1.90×10^{-14}	1.08×10^{-14}	5.68×10^{-15}
$\alpha_4 {}^2F^o$	1.09×10^{-14}	5.54×10^{-15}	2.56×10^{-15}
$\alpha_{10} {}^2S$	4.33×10^{-16}	2.84×10^{-16}	1.80×10^{-16}
$\alpha_{10} {}^2G$	2.02×10^{-15}	9.28×10^{-16}	3.91×10^{-16}
$\alpha_{10} {}^2M$	2.7×10^{-17}	1.0×10^{-17}	4.0×10^{-18}
α_A	6.82×10^{-13}	4.18×10^{-13}	2.51×10^{-13}
α_B	4.54×10^{-13}	2.59×10^{-13}	1.43×10^{-13}

the temperatures listed are of order $5 \times 10^7 \text{ cm s}^{-1}$, it can be seen that the recombination cross sections are of order 10^{-20} cm^2 or 10^{-21} cm^2 , much smaller than the geometrical cross section of an H atom.

In the nebular approximation discussed previously, recombination to any level $n {}^2L$ quickly leads through downward radiative transitions to $1 {}^2S$, and the total recombination coefficient is the sum over captures to all levels, ordinarily written

$$\begin{aligned}
 \alpha_A &= \sum_{n,L} \alpha_n {}^2L(\text{H}^0, T) [\text{cm}^3 \text{s}^{-1}] \\
 &= \sum_n \sum_{L=0}^{n-1} \alpha_{nL}(\text{H}^0, T) \\
 &= \sum_n \alpha_n(\text{H}^0, T)
 \end{aligned} \tag{2.7}$$

where α_n is thus the recombination coefficient to all the levels with principal quantum number n . Numerical values of α_A are also listed in Table 2.1. A typical recombination time is $\tau_r = 1/n_e \alpha_A \approx 3 \times 10^{12}/n_e \text{ s} \approx 10^5/n_e \text{ yr}$, and deviations from ionization equilibrium are ordinarily damped out in times of this order of magnitude.

2.3 Photoionization of a Pure Hydrogen Nebula

Consider the simple idealized problem of a single star that is a source of ionizing photons in a homogeneous static cloud of H. Only radiation with frequency $\nu \geq \nu_0$ is effective in the photoionization of H from the ground level, and the ionization equilibrium equation at each point can be written

$$n(\text{H}^0) \int_{\nu_0}^{\infty} \frac{4\pi J_\nu}{h\nu} a_\nu d\nu = n_p n_e \alpha_A(\text{H}^0, T) [\text{cm}^{-3} \text{s}^{-1}]. \quad (2.8)$$

The equation of transfer for radiation with $\nu \geq \nu_0$ can be written in the form

$$\frac{dI_\nu}{ds} = -n(\text{H}^0) a_\nu I_\nu + j_\nu \quad (2.9)$$

where I_ν is the specific intensity of radiation and j_ν is the local emission coefficient (in energy units per unit volume, per unit time, per unit solid angle, per unit frequency) for ionizing radiation.

It is convenient to divide the radiation field into two parts, a "stellar" part, resulting directly from the input radiation from the star, and a "diffuse" part, resulting from the emission of the ionized gas:

$$I_\nu = I_{\nu s} + I_{\nu d}. \quad (2.10)$$

The stellar radiation decreases outward because of geometrical dilution and absorption, and since its only source is the star, it can be written

$$4\pi J_{\nu s} = \pi F_{\nu s}(r) = \pi F_{\nu s}(R) \frac{R^2 \exp(-\tau_\nu)}{r^2} [\text{erg cm}^{-2} \text{s}^{-1} \text{Hz}^{-1}], \quad (2.11)$$

where $\pi F_{\nu s}(r)$ is the standard astronomical notation for the flux of stellar radiation (per unit area, per unit time, per unit frequency interval) at r , $\pi F_{\nu s}(R)$ is the flux at the radius of the star R , and τ_ν is the radial optical depth at r ,

$$\tau_\nu(r) = \int_0^r n(\text{H}^0, r') a_\nu dr', \quad (2.12)$$

which can also be written in terms of τ_0 , the optical depth at the threshold:

$$\tau_\nu(r) = \frac{a_\nu}{a_{\nu_0}} \tau_0(r)$$

The equation of transfer for the diffuse radiation $I_{\nu d}$ is

$$\frac{dI_{\nu d}}{ds} = -n(\text{H}^0) a_\nu I_{\nu d} + j_\nu \quad (2.13)$$

and for $kT \ll h\nu_0$ the only source of ionizing radiation is recaptures of electrons from the continuum to the ground 1^2S level. The emission coefficient for this radiation is $\text{erg cm}^{-3} \text{ s}^{-1} \text{ Hz}^{-1} \text{ sr}^{-1}$.

$$j_\nu(T) = \frac{2h\nu^3}{c^2} \left(\frac{h^2}{2\pi mkT} \right)^{3/2} a_\nu \exp[-h(\nu - \nu_0)/kT] n_p n_e \quad (\nu > \nu_0) \quad (2.14)$$

which is strongly peaked to $\nu = \nu_0$, the threshold. The total number of photons generated by recombinations to the ground level is given by the recombination coefficient

$$4\pi \int_{\nu_0}^{\infty} \frac{j_\nu}{h\nu} d\nu = n_p n_e \alpha_1(\text{H}^0, T) [\text{cm}^{-3} \text{ s}^{-1}], \quad (2.15)$$

and since $\alpha_1 = \alpha_{1s} < \alpha_A$, the diffuse field $J_{\nu d}$ is smaller than $J_{\nu s}$ on the average, and may be calculated by an iterative procedure. For an optically thin nebula, a good first approximation is to take $J_{\nu d} \approx 0$.

On the other hand, for an optically thick nebula, a good first approximation is based on the fact that no ionizing photons can escape, so that every diffuse radiation-field photon generated in such a nebula is absorbed elsewhere in the nebula:

$$4\pi \int \frac{j_\nu}{h\nu} dV = 4\pi \int n(\text{H}^0) \frac{a_\nu J_{\nu d}}{h\nu} dV, \quad (2.16)$$

where the integration is over the entire volume of the nebula. The so-called "on-the-spot" approximation amounts to assuming that a similar relation holds locally:

$$J_{\nu d} = \frac{j_\nu}{n(\text{H}^0) a_\nu} \quad (2.17)$$

This, of course, automatically satisfies (2.16), and would be exact if all photons were absorbed very close to the point at which they are generated ("on the spot"). This is not a bad approximation because the diffuse radiation-field photons have $\nu \approx \nu_0$, and therefore have large α_ν and correspondingly small mean free paths before absorption.

Making this on-the-spot approximation and using (2.11) and (2.15), we find that the ionization Equation (2.8) becomes

$$\frac{n(\text{H}^0) R^2}{r^2} \int_{\nu_0}^{\infty} \frac{\pi F_\nu(R)}{h\nu} a_\nu \exp(-\tau_\nu) d\nu = n_p n_e \alpha_B(\text{H}^0, T) \quad (2.18)$$

where

$$\begin{aligned} \alpha_B(\text{H}^0, T) &= \alpha_A(\text{H}^0, T) - \alpha_1(\text{H}^0, T) \\ &= \sum_2^{\infty} \alpha_n(\text{H}^0, T) \end{aligned}$$

The physical meaning is that in optically thick nebulae, the ionizations caused by stellar radiation-field photons are balanced by recombinations to excited levels of

Table 2.2
Calculated ionization distributions for model H II regions

r (pc)	$T_* = 4 \times 10^4$ K Blackbody Model		$T_* = 3.74 \times 10^4$ K Model stellar atmosphere	
	$\frac{n_p}{n_p + n(\text{H}^0)}$	$\frac{n(\text{H}^0)}{n_p + n(\text{H}^0)}$	$\frac{n_p}{n_p + n(\text{H}^0)}$	$\frac{n(\text{H}^0)}{n_p + n(\text{H}^0)}$
	0.1	1.0	4.5×10^{-7}	1.0
1.2	1.0	2.8×10^{-5}	1.0	2.9×10^{-5}
2.2	0.9999	1.0×10^{-4}	0.9999	1.0×10^{-4}
3.3	0.9997	2.5×10^{-4}	0.9997	2.5×10^{-4}
4.4	0.9995	4.4×10^{-4}	0.9994	4.5×10^{-4}
5.5	0.9992	8.0×10^{-4}	0.9992	8.1×10^{-4}
6.7	0.9985	1.5×10^{-3}	0.9985	1.5×10^{-3}
7.7	0.9973	2.7×10^{-3}	0.9973	2.7×10^{-3}
8.8	0.9921	7.9×10^{-3}	0.9924	7.6×10^{-3}
9.4	0.977	2.3×10^{-2}	0.979	2.1×10^{-2}
9.7	0.935	6.5×10^{-2}	0.940	6.0×10^{-2}
9.9	0.838	1.6×10^{-1}	0.842	1.6×10^{-1}
10.0	0.000	1.0	0.000	1.0

H, while recombinations to the ground level generate ionizing photons that are absorbed elsewhere in the nebula but have no net effect on the overall ionization balance.

For any stellar input spectrum $\pi F_\nu(R)$, the integral on the left-hand side of (2.18) can be tabulated as a known function of τ_0 , since a_ν and τ_ν are known functions of ν . Thus, for any assumed density distribution,

$$n_{\text{H}}(r) = n(\text{H}^0, r) + n_p(r)$$

and temperature distribution $T(r)$, equations (2.18) and (2.12) can be integrated outward to find $n(\text{H}^0, r)$ and $n_p(r) = n_e(r)$. Two calculated models for homogeneous nebulae with constant density $n(\text{H}) = 10$ H atoms plus ions cm^{-3} and constant temperature $T = 7,500$ K are listed in Table 2.2 and graphed in Figure 2.3. For one of these ionization models, the assumed $\pi F_\nu(R)$ is a blackbody spectrum with $T_* = 40,000$ K, chosen to represent approximately an O7.5 main-sequence star, while for the other, the $\pi F_\nu(R)$ is a computed model stellar atmosphere with $T_* = 37,450$ K. The table and graph clearly show the expected nearly complete ionization out to a critical radius r_1 , at which the ionization drops off abruptly to nearly zero. The central ionized zone is often referred to as an "H II region" ("H⁺ region" would be a better name), and it is surrounded by an outer neutral H⁰ region, often referred to as an "H I region".

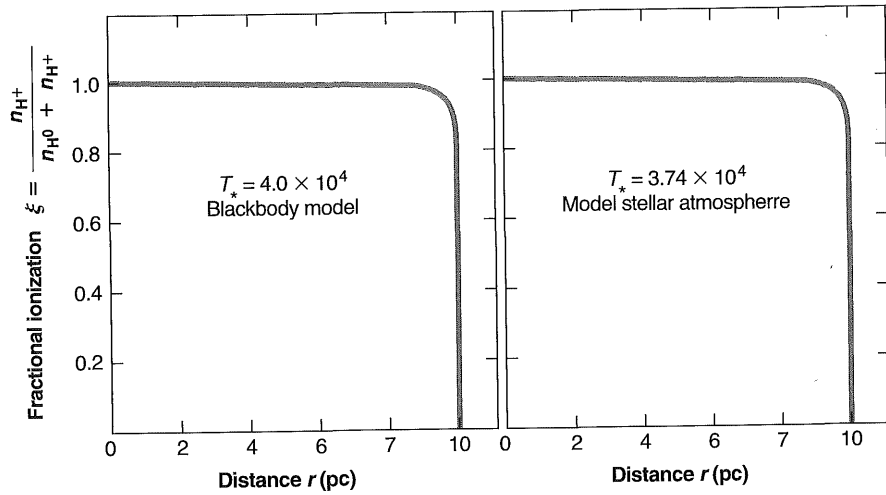


Figure 2.3
Ionization structure of two homogeneous pure-H model H II regions.

The radius r_1 can be found from (2.18), substituting from (2.12),

$$\frac{d\tau_\nu}{dr} = n(\text{H}^0) a_\nu$$

and integrating over r :

$$\begin{aligned} R^2 \int_{\nu_0}^{\infty} \frac{\pi F_\nu(R)}{h\nu} d\nu \int_0^{\infty} d[-\exp(-\tau_\nu)] &= \int_0^{\infty} n_p n_e \alpha_B r^2 dr \\ &= R^2 \int_{\nu_0}^{\infty} \frac{\pi F_\nu(R)}{h\nu} d\nu \end{aligned}$$

Using the result that the ionization is nearly complete [$n_p = n_e \approx n(\text{H})$] within r_1 , and nearly zero ($n_p = n_e \approx 0$) outside r_1 , this becomes

$$\begin{aligned} 4\pi R^2 \int_{\nu_0}^{\infty} \frac{\pi F_\nu}{h\nu} d\nu &= \int_{\nu_0}^{\infty} \frac{L_\nu}{h\nu} d\nu \\ &= Q(\text{H}^0) = \frac{4\pi}{3} r_1^3 n_{\text{H}}^2 \alpha_B. \end{aligned} \quad (2.19)$$

Here $4\pi R^2 \pi F_\nu(R) = L_\nu$ is the luminosity of the star at frequency ν (in energy units per time per unit frequency interval), and the physical meaning of (2.19) is that the total number of ionizing photons emitted by the star just balances the total number of recombinations to excited levels within the ionized volume $4\pi r_1^3$, often called the

Table 2.3
Calculated Strömgren radii as function of spectral types spheres

Spectral type	T_* (K)	M_V	$\log Q(\text{H}^0)$ (photons/s)	$\log Q(\text{He}^0)$ (photons/s)	$\log n_e n_p r_1^3$ n in cm^{-3} ; r_1 in pc	r_1 (pc) $n_e = n_p$ $= 1 \text{ cm}^{-3}$
O3 V	51,200	-5.78	49.87	49.18	6.26	122
O4 V	48,700	-5.55	49.70	48.99	6.09	107
O4.5 V	47,400	-5.44	49.61	48.90	6.00	100
O5 V	46,100	-5.33	49.53	48.81	5.92	94
O5.5 V	44,800	-5.22	49.43	48.72	5.82	87
O6 V	43,600	-5.11	49.34	48.61	5.73	81
O6.5 V	42,300	-4.99	49.23	48.49	5.62	75
O7 V	41,000	-4.88	49.12	48.34	5.51	69
O7.5 V	39,700	-4.77	49.00	48.16	5.39	63
O8 V	38,400	-4.66	48.87	47.92	5.26	57
O8.5 V	37,200	-4.55	48.72	47.63	5.11	51
O9 V	35,900	-4.43	48.56	47.25	4.95	45
O9.5 V	34,600	-4.32	48.38	46.77	4.77	39
B0 V	33,300	-4.21	48.16	46.23	4.55	33
B0.5 V	32,000	-4.10	47.90	45.69	4.29	27
O3 III	50,960	-6.09	49.99	49.30	6.38	134
B0.5 III	30,200	-5.31	48.27	45.86	4.66	36
O3 Ia	50,700	-6.4	50.11	49.41	6.50	147
O9.5 Ia	31,200	-6.5	49.17	47.17	5.56	71

Note: $T = 7,500$ K assumed for calculating α_B .

Strömgren sphere. Numerical values of radii calculated by using the model stellar atmospheres discussed in Chapter 5 are given in Table 2.3.

2.4 Photoionization of a Nebula Containing Hydrogen and Helium

The next most abundant element after H is He, whose relative abundance (by number) is of order 10 percent, and a much better approximation to the ionization structure of an actual nebula is provided by taking both these elements into account. The ionization potential of He is $h\nu_2 = 24.6$ eV, somewhat higher than H; the ionization potential of He^+ is 54.4 eV, but since even the hottest O stars emit practically no photons with $h\nu > 54.4$ eV, second ionization of He does not occur in ordinary H II regions. (The situation is quite different in planetary nebulae, as we shall see later in this chapter.) Thus photons with energy $13.6 \text{ eV} < h\nu < 24.6 \text{ eV}$ can ionize H only, but photons with energy $h\nu > 24.6 \text{ eV}$ can ionize both H and He. As a result, two different types of ionization structure are possible, depending on the spectrum of ionizing radiation and the abundance of He. At one extreme, if the spectrum is

concentrated to frequencies just above 13.6 eV and contains only a few photons with $h\nu > 24.6$ eV, then the photons with energy $13.6 \text{ eV} < h\nu < 24.6 \text{ eV}$ keep the H ionized, and the photons with $h\nu > 24.6 \text{ eV}$ are all absorbed by He. The ionization structure thus consists of a small central H^+ , He^+ zone surrounded by a larger H^+ , He^0 region. At the other extreme, if the input spectrum contains a large fraction of photons with $h\nu > 24.6 \text{ eV}$, then these photons dominate the ionization of both H and He, the outer boundaries of both ionized zones coincide, and there is a single H^+ , He^+ region.

The He^0 photoionization cross section $a_\nu(\text{He}^0)$ is plotted in Figure 2.2, along with $a_\nu(\text{H}^0)$ and $a_\nu(\text{He}^+)$ calculated from Equation (2.4). The total recombination coefficients for He to configurations $L \geq 2$ are, to a good approximation, the same as for H, since these levels are hydrogen-like, but because He is a two-electron system, it has separate singlet and triplet levels and

$$\left. \begin{aligned} a_n \text{ } ^1L(\text{He}^0, T) &\approx \frac{1}{4} \alpha_n \text{ } ^2L(\text{H}^0, T) \\ \alpha_n \text{ } ^3L(\text{He}^0, T) &\approx \frac{3}{4} \alpha_n \text{ } ^2L(\text{H}^0, T) \end{aligned} \right\} L \geq 2 \quad (2.20)$$

For the P and particularly the S terms there are sizeable differences between the He and H recombination coefficients. Representative numerical values of the recombination coefficients are included in Table 2.4.

The ionization equations for H and He are coupled by the radiation field with $h\nu > 24.6 \text{ eV}$, and are straightforward to write down in the on-the-spot approximation,

Table 2.4
Recombination coefficients (in $\text{cm}^3 \text{ s}^{-1}$) for He

	T		
	5,000 K	10,000 K	20,000 K
$\alpha(\text{He}^0, 1 \text{ } ^1S)$	2.17×10^{-13}	1.54×10^{-13}	1.10×10^{-13}
$\alpha(\text{He}^0, 2 \text{ } ^1S)$	7.62×10^{-15}	5.55×10^{-15}	4.07×10^{-15}
$\alpha(\text{He}^0, 2 \text{ } ^1P^o)$	1.97×10^{-14}	1.26×10^{-14}	7.57×10^{-15}
$\alpha(\text{He}^0, 3 \text{ } ^1S)$	2.20×10^{-15}	1.62×10^{-15}	1.19×10^{-15}
$\alpha(\text{He}^0, 3 \text{ } ^1P^o)$	7.87×10^{-15}	5.01×10^{-15}	2.99×10^{-15}
$\alpha(\text{He}^0, 3 \text{ } ^1D)$	7.53×10^{-15}	4.31×10^{-15}	2.26×10^{-15}
$\alpha_B(\text{He}^0, \sum n \text{ } ^1L)$	1.09×10^{-13}	6.23×10^{-14}	3.46×10^{-14}
$\alpha(\text{He}^0, 2 \text{ } ^3S)$	1.97×10^{-14}	1.49×10^{-14}	1.16×10^{-14}
$\alpha(\text{He}^0, 2 \text{ } ^3P^o)$	8.52×10^{-14}	5.60×10^{-14}	3.52×10^{-14}
$\alpha(\text{He}^0, 3 \text{ } ^3S)$	4.78×10^{-15}	3.72×10^{-15}	2.96×10^{-15}
$\alpha(\text{He}^0, 3 \text{ } ^3D)$	2.95×10^{-14}	1.95×10^{-14}	1.23×10^{-14}
$\alpha_B(\text{He}^0, \sum n \text{ } ^3L)$	3.57×10^{-13}	2.10×10^{-13}	1.21×10^{-13}
$\alpha_B(\text{He}^0)$	4.66×10^{-13}	2.72×10^{-13}	1.56×10^{-13}

though complicated in detail. First, the photons emitted in recombinations to the ground level of He can ionize either H or He, since these photons are emitted with energies just above $h\nu_2 = 24.6$ eV. The fraction absorbed by H is

$$y = \frac{n(\text{H}^0) a_{\nu_2}(\text{H}^0)}{n(\text{H}^0) a_{\nu_2}(\text{H}^0) + n(\text{He}^0) a_{\nu_2}(\text{He}^0)}, \quad (2.21)$$

and the remaining fraction, $1 - y$, is absorbed by He. Second, following recombination to excited levels of He, various photons are emitted that ionize H. Of the recombinations to excited levels of He, approximately three-fourth are to the triplet levels and approximately one-fourth are to the singlet levels. All the captures to triplets lead ultimately through downward radiative transitions to 2^3S , which is highly metastable, but which can decay by a one photon forbidden line at 19.8 eV to 1^1S , with transition probability $A(2^3S, 1^1S) = 1.26 \times 10^{-4} \text{ s}^{-1}$. Competing with this mode of depopulation of 2^3S , collisional excitation to the singlet levels 2^1S , and 2^1P^o can also occur with fairly high probability, while collisional transitions to 1^1S or to the continuum are less probable. Since the collisions leading to the singlet levels involve a spin change, only electrons are effective in causing these excitations, and the transition rate per atom in the 2^3S level is

$$n_e q(2^3S, 2^1L) = n_e \int_{\frac{1}{2}mu^2=\chi}^{\infty} u \sigma(2^3S, 2^1L, u) f(u) du \quad (2.22)$$

where the $\sigma(2^3S, 2^1L)$ are the electron collision cross sections for these excitation processes, and the χ are their energy thresholds. These rate coefficients are listed in Table 2.5, along with the critical electron density $n_c(2^3S)$, defined by

$$n_c(2^3S) = \frac{A(2^3S, 1^1S)}{q(2^3S, 2^1S) + q(2^3S, 2^1P^o)} \quad (2.23)$$

Table 2.5

Collisional rate coefficients (in $\text{cm}^3 \text{ s}^{-1}$) from $\text{He}^0(2^3S)$

$T(\text{K})$	$q(2^3S, 2^1S)$	$q(2^3S, 2^1P^o)$	n_c^a
6,000	1.95×10^{-8}	2.34×10^{-9}	6.2×10^3
8,000	2.45×10^{-8}	3.64×10^{-9}	4.6×10^3
10,000	2.60×10^{-8}	5.92×10^{-9}	3.9×10^3
15,000	3.05×10^{-8}	7.83×10^{-9}	3.3×10^3
20,000	2.55×10^{-8}	9.23×10^{-9}	3.3×10^3
25,000	2.68×10^{-8}	9.81×10^{-9}	3.4×10^3

a. Critical density in cm^{-3} .

at which collisional transitions are equally probable with radiative transitions. In typical H II regions, the electron density $n_e \leq 10^2 \text{ cm}^{-3}$, is considerably smaller than n_c , so practically all the atoms leave 2^3S by emission of a 19.8 eV-line photon. In contrast, in typical bright planetary nebulae, $n_e \approx 10^4 \text{ cm}^{-3}$, somewhat larger than n_c , and therefore many of the atoms are transferred to 2^1S or 2^1P^o before emitting a line photon. From the ratio of excitation rates, it can be seen that, for instance, at $T = 10^4 \text{ K}$, a fraction 0.83 of the transitions lead to 2^1S , and 0.17 to 2^1P^o . If the less probable collisional deexciting collisions to 1^1S are also included, these fractions become 0.78 and 0.16, respectively.

Of the captures to the singlet-excited levels in He, approximately two-thirds lead ultimately to population of 2^1P^o , while approximately one-third lead to population of 2^1S . Atoms in 2^1P^o decay mostly to 1^1S with emission of a resonance-line photon at 21.2 eV, but some also decay to 2^1S (with emission of $2^1S - 2^1P^o$ at $2.06 \mu\text{m}$) with a relative probability of approximately 10^{-3} . The resonance-line photons are scattered by He^0 , and therefore, after approximately 10^3 scatterings, a typical photon would, on the average, be converted to a $2.06\text{-}\mu\text{m}$ line photon and thus populate 2^1S . However, it is more likely that before a resonance-line photon is scattered this many times, it will photoionize an H atom and be absorbed. He atoms in 2^1S decay by two-photon emission (with the sum of the energies 20.6 eV and transition probability 51.3 s^{-1}) to 1^1S . From the distribution of photons in this continuous spectrum, the probability that a photon is produced that can ionize H is 0.56 per radiative decay from $\text{He}^0 2^1S$.

All these He bound-bound transitions produce photons that ionize H but not He, and they can easily be included in the H ionization equation in the on-the-spot approximation. The total number of recombinations to excited levels of He per unit volume per unit time is $n(\text{He}^+)n_e\alpha_B(\text{He}^0, T)$, and of these a fraction p generate ionizing photons that are absorbed on the spot. As shown by the preceding discussion, in the low-density limit $n_e \ll n_c$

$$p \approx \frac{3}{4} + \frac{1}{4} \left[\frac{2}{3} + \frac{1}{3} (0.56) \right] = 0.96,$$

but in the high-density limit $n_e \gg n_c$,

$$p \approx \left[\frac{3}{4} (0.78) + \frac{1}{4} \cdot \frac{1}{3} \right] (0.56) + \left[\frac{3}{4} (0.16) + \frac{1}{4} \cdot \frac{2}{3} \right] = 0.66.$$

Thus, in the on-the-spot approximation, the ionization equations become

$$\begin{aligned} \frac{n(\text{H}^0) R^2}{r^2} \int_{\nu_0}^{\infty} \frac{\pi F_{\nu}(R)}{h\nu} a_{\nu}(\text{H}^0) \exp(-\tau_{\nu}) d\nu + yn(\text{He}^+)n_e\alpha_1(\text{He}^0, T) \\ + pn(\text{He}^+)n_e\alpha_B(\text{He}^0, T) = n_p n_e \alpha_B(\text{H}^0, T); \end{aligned} \quad (2.24)$$

$$\frac{n(\text{He}^0) R^2}{r^2} \int_{\nu_2}^{\infty} \frac{\pi F_{\nu}(R)}{h\nu} a_{\nu}(\text{He}^0) \exp(-\tau_{\nu}) d\nu + (1-y) n(\text{He}^+) n_e \alpha_1(\text{He}^0, T) \quad (2.25)$$

$$= n(\text{He}^+) n_e \alpha_A(\text{He}^0, T),$$

with

$$\frac{d\tau_{\nu}}{dr} = n(\text{H}^0) a_{\nu}(\text{H}^0) \quad \text{for } \nu_1 < \nu < \nu_2$$

and

$$\frac{d\tau_{\nu}}{dr} = n(\text{H}^0) a_{\nu}(\text{H}^0) + n(\text{He}^0) a_{\nu}(\text{He}^0) \quad \text{for } \nu_2 < \nu, \quad (2.26)$$

and

$$n_e = n_p + n(\text{He}^+)$$

These equations again can be integrated outward step-by-step, and sample models for a diffuse nebula [with $n(\text{H}) = 10 \text{ cm}^{-3}$, $n(\text{He})/n(\text{H}) = 0.15$] excited by stars with $T_* = 40,000 \text{ K}$ and $30,000 \text{ K}$, respectively, are plotted in Figure 2.4. It can be seen that the hotter star excites a coincident H^+ , He^+ zone, while the cooler star has an inner H^+ , He^+ zone and an outer H^+ , He^0 zone.

Although the exact size of the He^+ zone can be found only from the integration because of the coupling between the H and He ionization by the radiation with $\nu > \nu_2$, the approximate size can easily be found by ignoring the absorption by H in the He^+ zone. This corresponds to setting $y = 0$ in Equation (2.25) and $n(\text{H}^0) = 0$ in the second of Equations (2.26), and we then immediately find, in analogy to Equation (2.19), that

$$\int_{\nu_2}^{\infty} \frac{L_{\nu}}{h\nu} d\nu = Q(\text{He}^0) = \frac{4\pi}{3} r_2^3 n(\text{He}^+) n_e \alpha_B(\text{He}^0), \quad (2.27)$$

where r_2 is the radius of the He^+ zone. Furthermore, since according to the preceding discussions, $p \approx 1$, the absorptions by He do not greatly reduce the number of photons available for ionizing H; therefore, to a fair approximation,

$$\int_{\nu_0}^{\infty} \frac{L_{\nu}}{h\nu} d\nu = Q(\text{H}^0) = \frac{4\pi}{3} r_1^3 n(\text{H}^+) n_e \alpha_B(\text{H}^0). \quad (2.19)$$

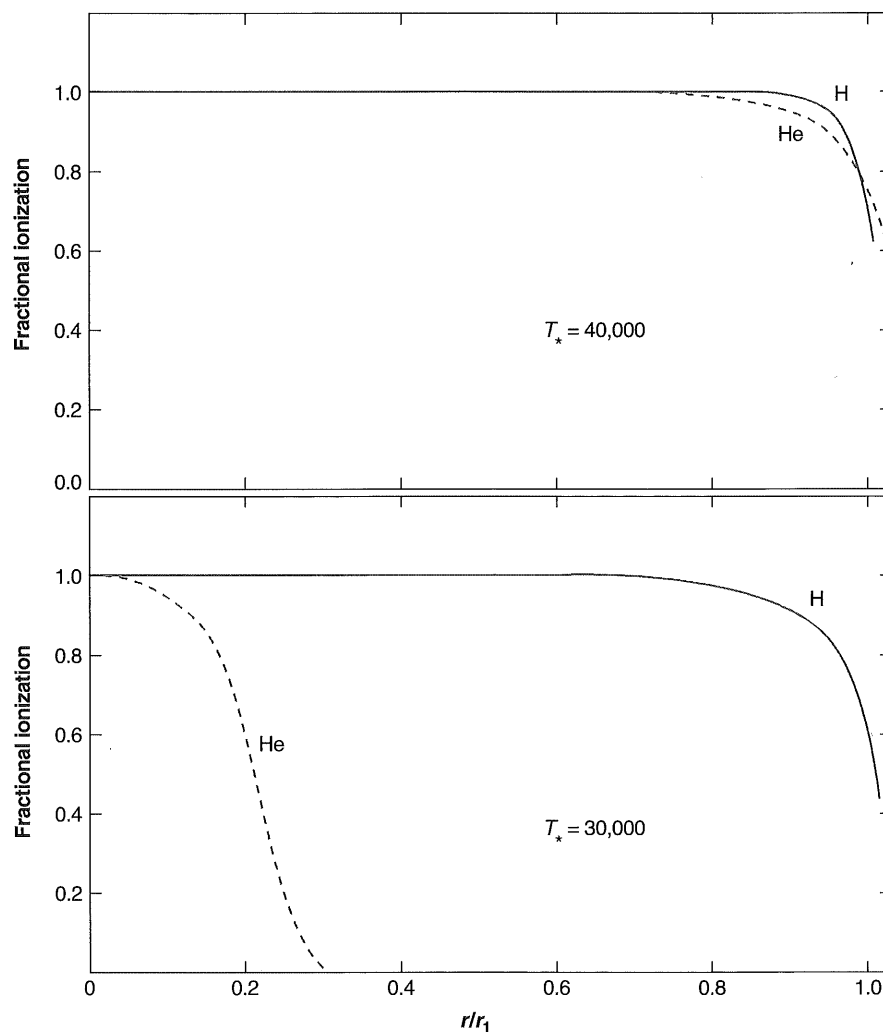


Figure 2.4
Ionization structure of two homogeneous $H^+ He$ model H II regions.

If we suppose that the He^+ zone is much smaller than the H^+ zone, then throughout most of the H^+ zone the electrons come only from ionization of H, but in the He^+ zone, the electrons come from ionization of both H and He. With this simplification,

$$\left(\frac{r_1}{r_2}\right)^3 = \frac{Q(H^0)}{Q(He^0)} \frac{n_{He}}{n_H} \left(1 + \frac{n_{He}}{n_H}\right) \frac{\alpha_B(He^0)}{\alpha_B(H^0)} \text{ if } r_2 < r_1. \quad (2.28)$$

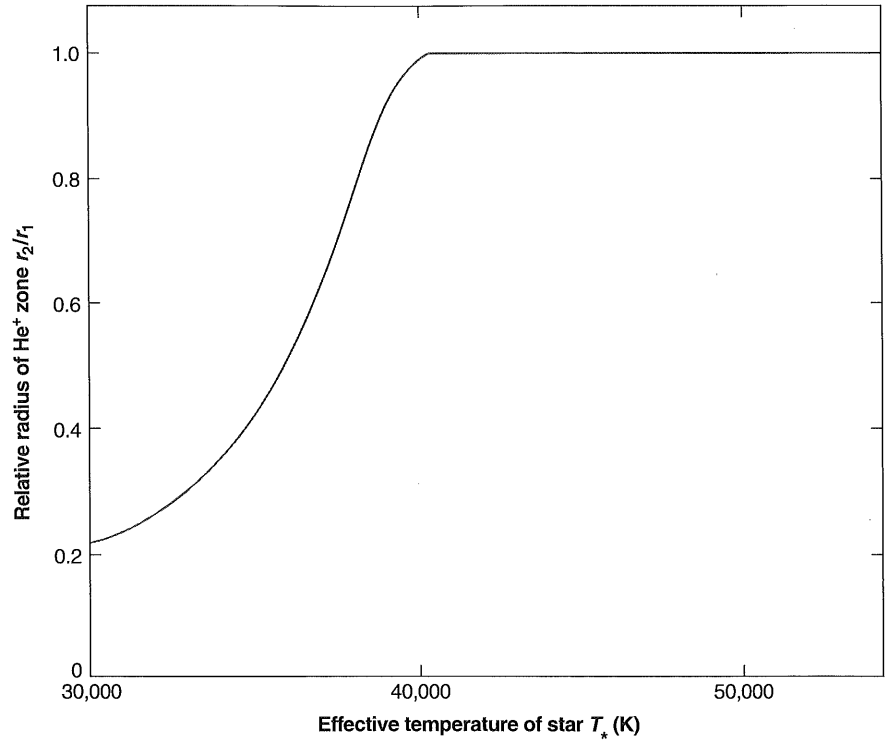


Figure 2.5

Relative radius of He^+ zone as a function of effective temperature of exciting star.

A plot of r_2/r_1 , calculated according to this equation for $n(\text{He})/n(\text{H}) = 0.15$ and $T = 7,500$ K, is shown in Figure 2.5, and it can be seen that, for $T_* \geq 40,000$ K, the He^+ and H^+ zones are coincident, while at significantly lower temperatures, the He^+ zone is much smaller. The details of the curve, including the precise effective temperature at which $r_2/r_1 = 1$, are not significant, because of the simplifications made, but the general trends it indicates are correct. For a smaller relative helium abundance, for instance $n(\text{He})/n(\text{H}) = 0.10$ instead of 0.15, r_2/r_1 is larger by approximately 16% at corresponding values of T_* , up to $r_2/r_1 = 1$.

2.5 Photoionization of He^+ to He^{++}

Although ordinary O stars of Population I do not radiate any appreciable number of photons with $h\nu > 54.4$ eV (hence galactic H II regions do not have a He^{++} zone), the situation is quite different for the central stars of planetary nebulae. Many of these stars are much hotter than even the hottest O3 stars, and do radiate high-energy photons

that produce central He^{++} zones, which are observed by the He II recombination spectra they emit.

The structure of these central He^{++} zones is governed by equations that are very similar to those for pure H^+ zones discussed previously, with the threshold, absorption cross section, and recombination coefficient changed from H^0 ($Z = 1$) to He^+ ($Z = 2$). This He^{++} zone is, of course, also an H^+ zone, and the ionization equations of H^0 and He^+ are therefore, in principle, coupled—but in practice they can be fairly well separated. The coupling results from the fact that, in the recombination of He^{++} to form He^+ , photons are emitted that ionize H^0 . Three different mechanisms are involved, namely: recombinations that populate 2^2P^o , resulting in He II $L\alpha$ emission with $h\nu = 40.8$ eV; recombinations that populate 1^2S , resulting in He II $2^2S \rightarrow 1^2S$ two-photon emission for which $h\nu' + h\nu'' = 40.8$ eV (the spectrum peaks at 20.4 eV, and, on the average, 1.42 ionizing photons are emitted per decay); and recombinations directly to 2^2S and to 2^2P^o , resulting in He II Balmer-continuum emission, which has the same threshold as the Lyman limit of H and therefore emits a continuous spectrum concentrated just above $h\nu_0$. The He II $L\alpha$ photons are scattered by resonance scattering, and therefore diffuse only slowly away from their point of origin before they are absorbed, while the He II Balmer-continuum photons are concentrated close to the H^0 ionization threshold and therefore have a short mean free path. Both these sources tend to ionize H^0 in the He^{++} zone, and at a “normal” abundance of He, the number of ionizing photons generated in the He^{++} zone by these two processes is nearly sufficient to balance the recombinations of H^+ in this zone and thus to maintain the ionization of H^0 . This is shown in Table 2.6, which lists the ionizing photon generation rates relative to the recombination rates for two temperatures. Thus, to a good approximation, the He II $L\alpha$ and Balmer-continuum photons are absorbed by and maintain the ionization of H^0 in the He^{++} zone, but the stellar radiation with $13.6 \text{ eV} < h\nu < 54.4 \text{ eV}$ is not significantly absorbed by the H^0 in the He^{++} , H^+ zone, and that with $h\nu > 54.4 \text{ eV}$ is absorbed only by the He^+ . The He II two-photon continuum is an additional source of ionizing photons for H; most of these photons escape from the He^{++} zone and therefore must be added to the stellar radiation field with $h\nu > 54.4 \text{ eV}$ in the He^+ zone. Of course, a more accurate calculation may be made, taking into account the detailed frequency dependence of

Table 2.6
Generation of H ionizing photons in the He^{++} zone

Number generated per H recombination	$T = 10,000 \text{ K}$	$20,000 \text{ K}$
$n(\text{He}^{++})q(\text{He}^+L\alpha)/n(\text{H}^+)\alpha_B(\text{H}^0)$	0.64	0.66
$n(\text{He}^{++})q(\text{He}^+ 2 \text{ photon})/n(\text{H}^+)\alpha_B(\text{H}^0)$	0.36	0.42
$n(\text{He}^{++})q(\text{He}^+B\alpha c)/n(\text{H}^+)\alpha_B(\text{H}^0)$	0.20	0.25

NOTE: Numerical values are calculated assuming that $n(\text{He}^{++})/n(\text{H}^+) = 0.15$.

each of the emission processes, but since normally the helium abundance is small, only an approximation to its effects is usually required.

Some sample calculations of the ionization structure of a model planetary nebula, with the radiation source a blackbody at $T_* = 10^5$ K are shown in Figure 2.6. The sharp outer edge of the He^{++} zone, as well as the even sharper outer edges of the H^+ and He^+ zones, can be seen in these graphs. There is, of course, an equation that is exactly analogous to (2.19) and (2.27) for the "Strömngren radius" r_3 of the He^{++} zone:

$$Q(\text{He}^+) = \int_{4\nu_0}^{\infty} \frac{L_\nu}{h\nu} d\nu = \frac{4\pi}{3} r_3^3 n(\text{He}^{++}) n_e \alpha_B(\text{He}^+, T) \quad (2.29)$$

Thus stellar temperatures $T_* \geq 10^5$ K are required for $r_3/r_1 \approx 1$.

2.6 Further Iterations of the Ionization Structure

As described previously, the on-the-spot approximation may be regarded as the first approximation to the ionization and, as will be described in Chapter 3, to the temperature distribution in the nebula. From these a first approximation to the emission coefficient j_ν may be found throughout the model: from j_ν a first approximation to $I_{\nu d}$ and hence J_ν at each point, and from J_ν a better approximation to the ionization and temperature at each point. This iteration procedure can be repeated as many times as desired (given sufficient computing time) and actually converges quite rapidly, but except where high accuracy is required, the first (on-the-spot) approximation is usually sufficient. The higher approximations show that the degree of ionization nearest the star is so high that ionizing photons emitted there are not really absorbed on the spot. There is thus a net flow of these photons from the center to the outer regions. However, the ionization calculated from the on-the-spot approximation is reasonably close to the final exact result.

2.7 Photoionization of Heavy Elements

Finally, let us examine the ionization of the heavy elements, of which O, C, Ne, N, Si, and Fe, with abundances (by number) of order 10^{-3} to 10^{-4} that of H, are the most abundant. The ionization–equilibrium equation for any two successive stages of ionization i and $i + 1$ of any element X may be written

$$\begin{aligned} n(X^{+i}) \int_{\nu_i}^{\infty} \frac{4\pi J_\nu}{h\nu} a_\nu(X^{+i}) d\nu &= n(X^{+i}) \Gamma(X^{+i}) \\ &= n(X^{+i+1}) n_e \alpha_G(X^{+i}, T), \end{aligned} \quad (2.30)$$

where $n(X^{+i})$ and $n(X^{+i+1})$ are the number densities of the two successive stages of ionization; $a_\nu(X^{+i})$ is the photoionization cross section from the ground level of X^i

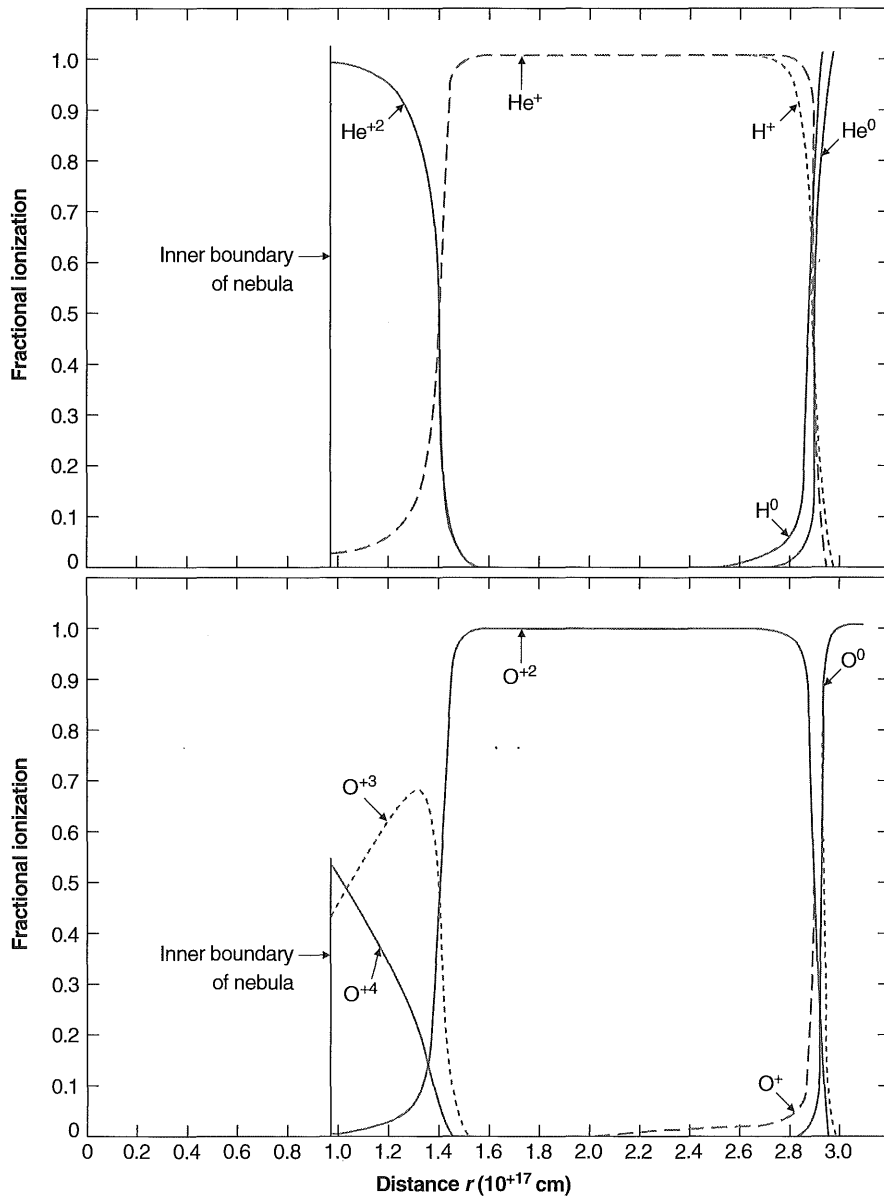


Figure 2.6 Ionization structure of H, He (top), and O (bottom) for a model planetary nebula.

with the threshold ν_i ; and $\alpha_G(X^{+i}, T)$ is the recombination coefficient of the ground level of X^{+i+1} to all levels of X^{+i} . These equations, together with the total number of ions of all stages of ionization,

$$n(X^0) + n(X^{+1}) + n(X^{+2}) + \dots + n(X^{+n}) = n(X)$$

(presumably known from the abundance of X), completely determine the ionization equilibrium at each point. The mean intensity J_ν , of course, includes both the stellar and diffuse contributions, but the abundances of the heavy elements are so small that their contributions to the diffuse field are negligible, and only the emission by H, He, and He^+ mentioned previously needs to be taken into account.

The heavy elements do not usually make an appreciable contribution to the optical depth, but in some situations they can, particularly at frequencies just below the He^0 threshold. They can always be included by simple generalizations of Equations (2.26),

$$\frac{d\tau_\nu}{dr} = n(\text{H}^0) a_\nu(\text{H}^0) + \sum_{X,i} n(X^{+i}) a_\nu(X^{+i}) \text{ for } \nu_0 < \nu < \nu_2 \quad (2.31)$$

and

$$\begin{aligned} \frac{d\tau_\nu}{dr} = & n(\text{H}^0) a_\nu(\text{H}^0) + n(\text{He}^0) a_\nu(\text{He}^0) \\ & + \sum_{X,i} n(X^{+i}) a_\nu(X^{+i}) \text{ for } \nu_2 < \nu \end{aligned}$$

In both these equations all stages of ionization of all heavy elements that have thresholds below the frequency for which the optical depth is being calculated are included in the sums over X and i .

Many ions of the heavy elements have one or more shells of electrons below the outer valence shell. Electrons within any shell can be removed when the source of ionizing radiation extends to high enough energies. The vacancies left by removal of inner electrons can be filled by outer electrons, producing emission lines at very high energies, or by the Auger effect, a multi-electron process where some electrons cascade down to fill the inner vacancy while others are ejected from the atom. Both processes are important contributors to the X-ray spectrum, and detailed discussion is presented in a later chapter, since here we are mainly concerned with nebulae photoionized by starlight.

The photoionization cross section of a particular shell behaves somewhat like the hydrogen and helium cross sections described above. The largest values are $\sim 10^{-18}$ – 10^{-17} cm^2 and often occur near the threshold, tending to decrease with increasing energy. Unlike H and He, there can also be many strong resonance features produced by interactions between various electrons.

Table 2.7
Recombination coefficients (in $\text{cm}^3 \text{s}^{-1}$) for H-like ions

	<i>T</i>				
	1,250 K	2,500 K	5,000 K	10,000 K	20,000 K
$\alpha_A = \sum_1^{\infty} \alpha_n$	1.74×10^{-12}	1.10×10^{-12}	6.82×10^{-13}	4.18×10^{-13}	2.51×10^{-13}
$\alpha_B = \sum_2^{\infty} \alpha_n$	1.28×10^{-12}	7.72×10^{-13}	4.54×10^{-13}	2.59×10^{-13}	1.43×10^{-13}
$\alpha_C = \sum_3^{\infty} \alpha_n$	1.03×10^{-12}	5.99×10^{-13}	3.37×10^{-13}	1.87×10^{-13}	9.50×10^{-14}
$\alpha_D = \sum_4^{\infty} \alpha_n$	8.65×10^{-13}	4.86×10^{-13}	2.64×10^{-13}	1.37×10^{-13}	6.83×10^{-14}

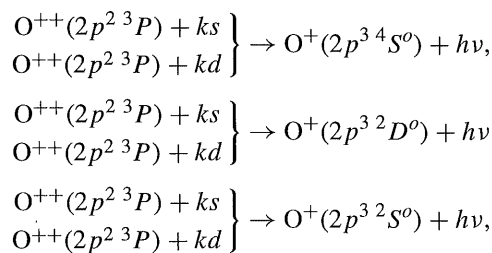
NOTE: In this table $Z = 1$; for other values of Z , $\alpha(Z, T) = Z\alpha(1, T/Z^2)$.

The recombination coefficients for complex ions may be divided into radiative and dielectronic parts,

$$\alpha_G(X^{+i}, T) = \alpha_R(X^{+i}, T) + \alpha_d(X^{+i}, T). \quad (2.32)$$

The radiative part represents simple bound-free recaptures. Just as in H and He, captures to any level are followed by downward radiative transitions, leading ultimately to the ground level. Thus the radiative recombination coefficient is a sum over all levels, and is dominated by the excited levels, which to a good approximation are hydrogen-like (Table 2.7 gives these).

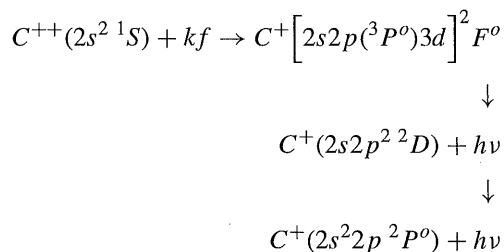
In the best calculations, the deviations due to departures of the energy levels from the exact hydrogen-like energies must be taken into account. The recombinations to the terms resulting from recaptures of an electron to the innermost unfilled shell, for instance,



are strongly affected by the presence of the other bound electrons, through the Pauli principle, and are far from hydrogen-like. These recombination coefficients can be found from the computed photoionization cross sections, using the Milne relation as explained in Appendix 2.

The additional dielectronic part of the recombination coefficient is larger than the radiative part for many, but not all, heavy ions at nebular temperatures. It results from resonances (at specific energies) in the total recombination cross sections, which are related to resonances (at related specific frequencies) in the corresponding photoionization cross section. Physically, these occur at energies at which the incoming free electron can give up nearly all its kinetic energy to exciting a bound level of the ion, thus creating a short-lived doubly excited level of the next lower stage of ionization. This level can then often decay to a singly excited bound level, and then by further successive radiative transitions downward to the ground level.

An example is the recombination of C^{++} to form C^+ . A free electron with kinetic energy 0.41 eV colliding with a C^{++} ion in the ground $2s^2\ ^1S$ level makes up a five-electron system with the same total energy as a C^+ ion in the $2s2p3d\ ^2F^o$ term. There is thus a strong resonance centered at this energy, representing the high probability of collisional excitation of one of the bound $2s$ electrons to $2p$ together with capture of the free electron into the $3d$ shell. This term can then emit a photon decaying with non-zero transition probability to $2s2p^2\ ^2D$, a bound term, which decays ultimately to the ground $2s^22p\ ^2P_{1/2}$ level. This dielectronic transition process may be written



This is actually the main recombination process for C^{++} at nebular temperatures. Note that spin, orbital angular momentum, and parity must all be conserved in the first radiationless transition; for this reason, only free f ($l = 3$) electrons are involved in this specific dielectronic recombination process.

In addition, there is a third contribution, the integrated effect of many higher-energy resonances, which is ordinarily small at nebular temperatures. It can have a non-zero effect, and should be included in the most accurate calculations.

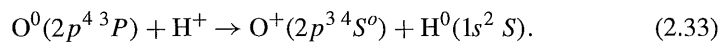
Selected calculated values of $\alpha(X^{+i}, T)$ are listed in Appendix 5 in Tables A5.1 (for ions present in nebulae) and A5.2 (for ions present in X-ray sources such as AGN). The temperature dependence is not simple, because the resonance effects introduce an exponential behavior, so the values are given at three representative temperatures. Dielectronic recombination is more important in some situations, but radiative recombination is more important at others. For most but not all of these ions the importance of dielectronic recombination grows with increasing temperature. Both recombination processes must be taken into account in all calculations.

Calculations have been made of the ionization of heavy elements in many model H II regions and planetary nebulae. In H II regions, the common elements, such

as O^+ and N^+ , tend to be mostly singly ionized in the outer parts of the nebulae, although near the central stars there are often fairly large amounts of O^{++} , N^{++} , and Ne^{++} . Most planetary nebulae have hotter central stars, and the degree of ionization is correspondingly higher. This is shown in Figure 2.6, where the ionization of O is plotted for a calculated model planetary nebula. Note that in this figure the outer edge of the He^{++} zone is also the outer edge of the O^{+3} zone and the inner edge of the O^{++} zone, since O^{++} has an ionization potential 54.9 eV, nearly the same as He^+ .

Again, in actual nebulae, density condensations play an important role in complicating the ionization structure; these simplified models do, however, give an overall picture of the ionization.

One other atomic process is important in determining the ionization equilibrium of particular light elements, especially near the outer boundaries of radiation-bounded nebulae. This process is charge exchange in two-body reactions with hydrogen. As an example, consider neutral oxygen, which has the charge-exchange reaction with a proton



This reaction converts an originally neutral O atom into an O^+ ion, and thus is an ionization process for O. There is an attractive polarization force between O^0 and H^+ ; in addition, the ionization potentials of O and H are very nearly the same, so that the reaction is very nearly a resonance process. For both of these reasons the cross section for this charge-exchange reaction is relatively large. The reaction rate per unit volume per unit time for the reaction can be written

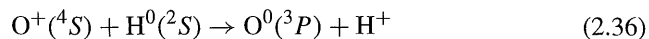
$$n_O n_p \delta(T) \text{ [cm}^{-3} \text{ s}^{-1}\text{]}, \quad (2.34)$$

where $\delta(T)$ is expressed in terms of the reaction cross section $\sigma(u)$ by an integral analogous to Equation (2.5),

$$\delta(T) = \int_0^\infty u \sigma(u) f(u) du. \quad (2.35)$$

Here it should be noted that $f(u)$ is the Maxwell-Boltzmann distribution function for the relative velocity u in the OH^+ center-of-mass system, and thus involves their reduced mass.

A selection of computed values of $\delta(T)$ for many ions is given in Tables A5.3 and A5.4. We concentrate on O because of its importance. For instance, in an H II region with $n_p = 10 \text{ cm}^{-3}$, the ionization rate per O atom per unit time is about 10^{-8} s^{-1} , comparable with the photoionization rate for the typical conditions adopted in Section 2.1. Likewise, the rate for the inverse reaction



can be written

$$n(O^+)n(H^0)\delta'(T).$$

Numerical values of $\delta'(T)$, which of course is related to $\delta(T)$ through an integral form of the Milne relation

$$\frac{\delta'}{\delta} = \frac{9}{8} \exp(\Delta E/kT) \quad (2.37)$$

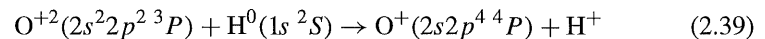
where $\Delta E = 0.0196$ eV is the difference in the ionization potentials of O^0 and H^0 , are given for O^+ and several other ions in Table A5.4. Comparison of Table A5.4 with Table A5.1 shows that charge exchange has a rate comparable with recombination in converting O^+ to O^0 at the typical H II region conditions, but at the outer edge of the nebula, charge exchange dominates because of the higher density of H^0 . At the higher radiation densities that occur in planetary nebulae, charge exchange is not important in the ionization balance of O except near the outer edge of the ionized region. The charge-exchange reactions do not appreciably affect the ionization equilibrium of H, because of the low O and O^+ densities.

At temperatures that are high compared with the difference in ionization potentials between O^0 and H^0 , the charge-exchange reactions (2.33) and (2.36) tend to set up an equilibrium in which the ratio of species depends only on the statistical weights, since $\delta'/\delta \rightarrow 9/8$. It can be seen from Tables A5.3 and A5.4 that this situation is closely realized at $T = 10,000$ K. Thus in a nebula, wherever charge-exchange processes dominate the ionization balance of O, its degree of ionization is locked to that of H by the equation

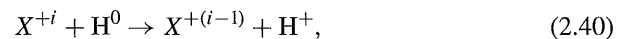
$$\frac{n(O^0)}{n(O^+)} = \frac{9}{8} \frac{n(H^0)}{n_p} \quad (2.38)$$

Thus high densities of O^0 and free electrons exist together only in the edges or transition zone of the ionized region, as shown in Figure 2.6. Dense neutral condensations within planetary nebulae therefore show strong [OI] emission, as seen in Figure 2.7.

Another type of charge-exchange reaction that can be important in the ionization balance of heavy ions is exemplified by



Note that the O^+ is left in an excited state. This reaction is strongly exothermic, with an energy difference $\Delta E = 6.7$ eV. In addition, there are almost no $O^+(2s 2p^4 \ ^4P)$ ions (with excitation energy 14.9 eV) present in the nebula. Hence the inverse reaction, which has this threshold, essentially does not proceed at all at nebular temperatures. Reaction (2.39) and some others like it, have large cross sections because it is a two-body process for which the strong Coulomb repulsion of the products speeds up the process. For the general reaction



the rate per unit volume per unit time may be written

$$n(X^{+i})n(H^0)\delta'(T),$$

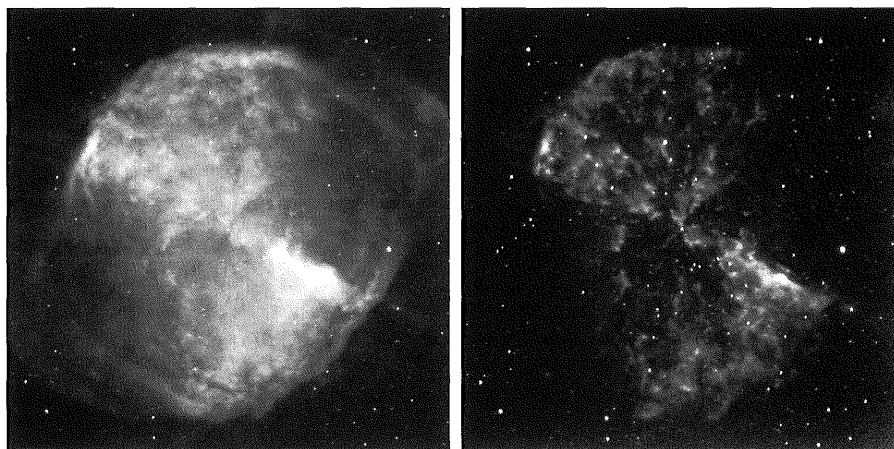


Figure 2.7

Monochromatic images of the planetary nebula NGC 6853 in the light of $H\alpha + [N II]$ (left) and in the light of $[O I] \lambda 6300$ (right). Note that, in contrast with $H\alpha$, the $[O I]$ emission is strongly concentrated to many bright spots, which are high-density neutral condensations (surrounded by partly ionized edges in which both O^0 and free electrons are present). (George Jacoby/WIYN/NSF)

and calculated values of $\delta'(T)$ are listed for three temperatures in Table A5.4. As the table shows, several of these rate coefficients are quite large. Thus even though the density of H^0 is small in comparison with the electron density, these charge-exchange reactions can be as important as recombination, or even more so, in determining the ionization equilibrium for these heavy ions. Similar charge reactions with He^0 , and even between two heavy elements, can also make appreciable contributions to the ionization balance, and these should be included in any complete calculation.

References

Much of the early work on gaseous nebulae was done by H. Zanstra, D. H. Menzel, L. H. Aller, and others. The very important series of papers on physical processes in gaseous nebulae by D. H. Menzel and his collaborators is collected in *Selected Papers on Physical Processes in Ionized Nebulae* (New York: Dover) 1962. The treatment in this chapter is based on ideas that were, in many cases, given in these pioneering papers. The specific formulation and the numerical values used in this chapter are largely based on the references listed here.

Basic papers on ionization structure:

Strömngren, B. 1939, *ApJ*, 89, 529.

Hummer, D. G., & Seaton, M. J. 1963, *MNRAS*, 125, 437.

Hummer, D. G., & Seaton, M. J. 1964, *MNRAS*, 127, 217.

The name "Strömgren sphere" comes from the first of these papers, the pioneering basic treatment that began the theoretical understanding of H II regions.

Numerical values of H recombination coefficient:

Seaton, M. J. 1959, MNRAS, 119, 81.

Burgess, A. 1964, Mem. RAS, 69, 1.

Pengelly, R. M. 1964, MNRAS, 127, 145.

Hummer, D. G., & Storey, P. J. 1987, MNRAS, 224, 80.

Storey, P. J., & Hummer, D. G. 1995, MNRAS, 272, 41 (on the web at <http://adc.gsfc.nasa.gov/adc-cgi/cat.pl?/catalogs/6/6064/>).

(Tables 2.1, 2.6, and 2.7 are based on these references.)

Numerical values of He recombination coefficient:

Burgess, A., & Seaton, M. J. 1960, MNRAS, 121, 471.

Robbins, R. R. 1968, ApJ, 151, 497.

Robbins, R. R. 1970, ApJ, 160, 519.

Brown, R. L., & Mathews, W. G. 1970, ApJ, 160, 939.

Verner, D. A., & Ferland, G. J. 1996, ApJS, 103, 467.

Smits, D. P. 1996, MNRAS, 278, 683.

Benjamin, R. A., Skillman, E. D., & Smits, D. P. 1999, ApJ, 514, 307.

(Table 2.4 is based on the last two references.)

The calibration of the spectral classes in terms of effective temperature and number of ionizing photons is discussed by

Morton, D. C. 1969, ApJ, 158, 629.

Panagia, N. 1973, AJ, 78, 929.

Vacca, W. D., Garmany, C. D., & Shull, J. M. 1996, ApJ, 460, 914.

Schaerer, D., & de Koter, A. 1997, A&A, 322, 598.

Sternberg, A., Hoffman, T. L., & Pauldrach, A. W. A. 2003, ApJ, 599, 1333.

Table 2.3 comes from the third of these references. There are only minor differences between them and the somewhat later numerical values in the last reference. These differences are especially small for the hottest and most luminous objects.

Numerical values of He ($2^3S \rightarrow 2^1S$ and 2^1P) collisional cross sections:

Bray, I., Burgess, A., Fursa, D. V., & Tully, J. A. 2000, A&AS, 146, 481.

Table 2.5 is based on this reference. It also gives collisional excitation rates to levels $n = 3, 4,$ and 5 , which are negligible at low temperatures and make at most a 10 percent correction at the highest temperature in Table 2.5.

Numerical values of the H and He⁺ photoionization cross sections:

Hummer, D. G., & Seaton, M. J. 1963, MNRAS, 125, 437.

(Figure 2.2 is based on this reference and the following ones.)

Numerical values of the He photoionization cross section:

Bell, K. L., & Kingston, A. E. 1967, *Proc. Phys. Soc.*, 90, 31.

Brown, R. L. 1971, *ApJ*, 164, 387.

Hummer, D. G., & Storey, P. J. 1998, *MNRAS*, 297, 1073.

Numerical values of He ($2^1S \rightarrow 1^1S$) and He ($2^3S \rightarrow 1^1S$) transition probabilities, including the frequency distribution in the $2^1S \rightarrow 1^1S$ two photon spectrum:

Lin, C. D., Johnson, W. R., & Dalgarno, A. 1977, *Phys Rev A*, 15, 154.

Drake, G. W. F. 1979, *Phys Rev A*, 19, 1387.

Hata, J., & Grant, I. P. 1981, *J Phys B*, 14, 2111.

Lach, G., & Pachucki, K. 2001, *Phys Rev A*, 64, 42510.

Early calculations of model H II regions:

Hjellming, R. M. 1966, *ApJ*, 143, 420.

Rubin, R. H. 1968, *ApJ*, 153, 761.

Rubin, R. H. 1983, *ApJ*, 274, 671.

(Figure 2.4 is based on the second of these references. The last emphasizes the importance of heavy-element opacity in some situations.)

Early calculations of model planetary nebulae:

Harrington, J. P. 1969, *ApJ*, 156, 903.

Flower, D. R. 1969, *MNRAS*, 146, 171.

Harrington, J. P. 1979, *Planetary Nebulae, Observations and Theory* (IAU Symposium No. 76), ed. Y. Terzian (Dordrecht: Reidel), p. 15.

(Figure 2.6 is based on the second of these references.)

References to other later, still more detailed models of H II regions and planetary nebulae are given in Chapter 5.

Dense neutral condensations in planetary nebulae are discussed by

O'Dell, C. R., Henney, W. J., & Burkert, A. 2000, *AJ*, 119, 2910.

O'Dell, C. R., 2000, *AJ*, 119, 2311.

Model atmospheres for hot stars are discussed in more detail in Chapter 5. In the present chapter, it is easiest to say that the simplest models are blackbodies; a much better approximation is provided by models in which the continuous spectrum is calculated; and the best models are those that also include the effects of the absorption lines, since they are strong and numerous in the ultraviolet, as well as winds.